Higgs boson production via new vector-like top quark decays and detection in diphoton or multilepton plus multijets channels at the LHC

A. Azatov,[1] O. Bondu,[2] A. Falkowski,[3] M. Felcini,[4] S. Gascon-Shotkin,[2]
D. K. Ghosh,[5] G. Moreau,[3] A. Y. Rodríguez-Marrero,[4] and S. Sekmen[6]

[1] *Dipartimento di Fisica, Università di Roma "La Sapienza", INFN Sezione, I-00185 Roma, Italy*
[2] *Université de Lyon, Université Claude Bernard Lyon 1, CNRSIN2P3, Institut de Physique Nucléaire de Lyon, F-69622 Villeurbanne Cedex, France*
[3] *Laboratoire de Physique Théorique, Bât. 210, CNRS, Université Paris 11, F-91405 Orsay Cedex, France*
[4] *Instituto de Física de Cantabria (IFCA), CSIC-Universidad de Cantabria, E-39005 Santander, Spain*
[5] *Department of Theoretical Physics, Indian Association for the Cultivation of Science Kolkata 700 032, India*
[6] *CERN Physics Department, CH-1211 Geneva 23, Switzerland.*

Motivated by the recent stringent constraints from the search for direct Higgs boson production at the LHC, over a wide Higgs mass range, we first build a minimal model of vector-like quarks where the dominant Higgs production process at the LHC, via gluon fusion, can be significantly suppressed. Within this model, compatible with the present experimental constraints, we demonstrate that the Higgs production via a heavy vector-like quark, t_2, decay, $pp \to t_2\bar{t}_2$, $t_2 \to th$, allows to discover a Higgs boson and measure its mass, through the decay channels $h \to \gamma\gamma$ or $h \to ZZ$. We also comment on the recent hint in LHC data from a possible ~ 125 GeV Higgs, in the presence of heavy vector-like top quarks.

PACS numbers:

I. INTRODUCTION

One of the primary goals of the Large Hadron Collider (LHC) is the direct search for the cornerstone of the Standard Model (SM), namely the Higgs boson, or of any signal from alternative Electro-Weak Symmetry Breaking (EWSB) mechanisms. The SM is probably not the ultimate model of nature. It is clear that new channels for Higgs production, that can arise in extensions of the SM, would have profound impact on the discovery of a Higgs boson, while providing insight in the physics beyond the SM. An attractive possibility is the Higgs production in decays of additional heavy colored particles as those can be copiously pair produced at the LHC via strong interactions.

Within well-motivated theories beyond the SM, there are some candidates for such new heavy colored states, extra quarks with vector-like couplings, whose existence is predicted by most of the alternatives to supersymmetry. In this context, to maintain a naturally light Higgs boson, divergent quantum corrections from loops of the top quark are often canceled by top-partner contributions [1–3]. Let us describe important examples here. In the so-called little Higgs scenarios, the vector-like quarks arise as partners of the SM fields being promoted to larger multiplets. In the composite Higgs [4–8] and composite top [4–9] models, the vector-like quarks are excited resonances of the bounded states constituting the SM particles. In the extra-dimensional models with (SM) quarks in the bulk, the vector-like quarks are prevalent as Kaluza-Klein (KK) excitations of those bulk fields [10] like in the Gauge-Higgs unification mechanism (see e.g. Ref. [11, 12]) or in the Randall-Sundrum (RS) scenario [13–15] – where some of those KK excitations, the so-called custodians, can be as light as a few hundred's of GeV [16–21]. Another example is a gauge coupling unification theory where vector-like quarks are embedded into the simplest SU(5) representations [22].

Vector-like quarks with same electric charge as the up-type quarks are often called top-partners (noted t') as these new heavy states mix in general predominantly with the top quark – due to the large top mass and to the related feature that the top quark is in general more intimately connected to ultraviolet physics, like e.g. in composite Higgs models. A t' can also be called a top-partner in the sense that it is contained in the same group representation as the top quark with respect to symmetries, like the approximate global symmetry of the little Higgs models [1–3], the gauge unification symmetry [22] or the custodial symmetry of RS versions with bulk matter [16–21] (explaining the SM fermion mass hierarchies [23–37]).

At this level, one must mention that the phenomenology of the search for direct production of vector-like quarks at the LHC has been studied from a model-independent point of view in Ref. [38–43] but also in specific frameworks such as the little Higgs models (versions sufficiently safe from EW precision constraints) [44–48] or the composite Higgs hypothesis [49, 50] and the dual RS context [11, 51–56]. These past searches focus generally on the discovery of the vector-like quarks, rather than using these extra quarks to enhance the discovery and identification potential for other unknown particles such as Higgs scalars.

In relation to Higgs detection, there exist studies utilizing the possible Higgs production through vector-like quark decays, as described in the following. Indeed, it is well known since some time [57, 58] that vector-like quark production could be a copious source of Higgs bosons (a possible Higgs factory).

Relatively light Higgs bosons produced from the decay of top-partners can be highly boosted and good candidates for analyses based on jet substructure. This method has been applied [59] for a $\sim$130 GeV Higgs decaying to $b\bar{b}$

at the 14 TeV LHC. In the simple model considered there, the t' is a singlet under the $SU(2)_L$ gauge group, which determines the t' couplings and its tree level decays into the Higgs boson and the two EW gauge bosons $t' \to th$, $t' \to tZ$, $t' \to bW$.
The top-partner can also be singly produced which leads to different final states as compared to the pair production; because of the phase space suppression, the single production becomes competitive with the pair production at a high t' mass, depending upon the considered model (since the involved t' couplings to $h, Z^0, W^\pm$ are fixed by the t' quantum numbers) [93]. The reconstruction of the Higgs boson produced in the t' decay, itself singly produced at the 14 TeV LHC, was studied in Ref. [60] assuming the Higgs mass known (to be 120 GeV) and focusing on the channel $h \to b\bar{b}$ – with the combinatorial background only. This was performed for a singlet t' in the "Littlest Higgs" model with the asymptotic branching ratio values of the high $m_{t'}$ regime: $B_{t' \to th} = 25\%$, $B_{t' \to tZ} = 25\%$, $B_{t' \to bW} = 50\%$ (from the EW equivalence theorem).
Similarly, a vector-like colored b' state produced at the 14 TeV LHC can act as a Higgs factory thanks to its decay $b' \to bh$. It was shown [22] that a Higgs mass reconstruction can be obtained with a limited accuracy, concentrating on the decay $h \to WW$ ($W \to l\nu$) for $m_h = 200$ GeV and assuming the $m_{b'}$ value to be deduced from a preliminary analysis based on the more appropriate channel $b' \to bZ$. Theoretically, the b' was originating from the upper component of a $SU(2)_L$ doublet so there was no significant channel $b' \to tW$.
Higgs mass reconstructions via t' and b' decays were also studied for the 14 TeV LHC, based on a light Higgs decaying to $b\bar{b}$ in the basic models with a unique extra t' and/or a unique extra b' [42].

In the present paper, we use the pair production and decay of a vector-like top to develop new search strategies for Higgs boson discovery and mass measurements in the $h \to \gamma\gamma$ (diphoton) and $h \to ZZ$ channels. We consider t' masses up to ~ 800 GeV, so that the t' single productions (involving a model-dependent coupling) are generally subleading compared to the t' pair production not yet significantly suppressed by phase space factors [94]. The original theoretical model considered here, including two top-partners, is constructed to allow interesting interpretations correlating the indirect (via vector-like top decay) and direct Higgs production searches at the LHC, as described in the following. A few characteristic parameter sets – with vector-like top mass in the range between ~ 400 and 800 GeV – are chosen as benchmark points avoiding too large t' contributions to the Higgs rates (constrained by present LHC data) and simultaneously allowing for significant branching fraction values ($\gtrsim 10\%$) of the vector-like top decay to the Higgs boson.
Assuming the presence at low-energy scales only of extra vector-like quark multiplets containing some t', we have elaborated a minimal model allowing to strongly suppress the Higgs production via gluon fusion, as compared to the SM. In this simple but non-trivial model, the $gg \to h$ cross section suppression factor possibly reaches values below 10^{-1} at hadron colliders; this is to be put in contrast with the t' representations taken usually in the RS scenario [21, 61–64] [95] and with minimal supersymmetric theories for which such a suppression is not possible to get (see respectively Ref. [21, 61] and Ref. [65]). The chiral case of a fourth quark generation can even only increase considerably the gluon fusion rate.
The minimal t' model suggested here is interesting in the sense that it can easily lead to the following interpretations: for example, a 255 GeV Higgs is excluded in the SM by the present LHC results [66, 67] but can still exist in the above minimal SM extension with t' where the reduced Higgs production cross section can be below the LHC upper limits. In other words, the Higgs boson would really be light but not detectable with the present luminosity/energy, via conventional channels. A channel that could then allow the Higgs discovery would be through the t' pair production and decays, as illustrated in this paper. Another possibility is that the slight excess of events observed in data for a Higgs mass hypothesis of $\sim$125 GeV [68, 69] is confirmed at the LHC. Then the measured Higgs production cross section times branching ratios could certainly be reproduced by the present t' model, given the parameter freedom in this model and its capability of inducing large Higgs rate corrections of both signs. Then investigating such another Higgs production channel as the t' decay, as developed here, would of course be relevant in particular to confirm the Higgs existence. Finally, in the case of a signal from a heavy Higgs, say above 500 GeV [96] as we will look at here, the same fit of Higgs data would be instructive as a test of the present t' model and similarly the t' decay should be considered as a complementary channel of Higgs production.

II. THE THEORETICAL MODEL

At low scale, let us assume the presence of a unique additional vector-like quark multiplet including a t' component. Then, irrespective of the representation of this multiplet under the $SU(2)_L$ gauge group (i.e. the t' belongs to a singlet, doublet,...), the interferences between the next heavier top mass eigenstate t_2 [composed of t, t', t''] and the t_1 [$\equiv$ the physical top quark whose mass is measured] contributions [97] to the triangular loop of the gluon-gluon fusion mechanism will be systematically constructive. This is due to the fact that the physical signs of the Yukawa coupling and mass insertion involved in this loop – two chirality flips are necessary – will be systematically identical giving rise to a positive product (for t_1 as well as for t_2). Hence, the cross section of the gluon fusion mechanism may be increased or slightly decreased (because of a possible t Yukawa coupling reduction) relatively to the SM case.
To get the minimal scenario with only additional vector-like quark multiplets including t' components able to strongly

suppress the gluon fusion, one needs to introduce a first top-partner t' in a $\mathrm{SU(2)_L}$ doublet as well as a second top-partner t'' in a gauge singlet. For simplification, we do not consider the doublet including a b' [98] that would also be exchanged in the triangular loop. So we end up with the doublet $(q_{5/3}, t')$, $q_{5/3}$ being an exotic quark with electric charge 5/3 and without self-Yukawa coupling (in turn no possible loop exchange). Indeed, with this field content, all the possible generic mass terms and Yukawa couplings appearing in the Lagrangian are,

$$\mathcal{L}_{\text{Yuk.}} = Y\overline{\begin{pmatrix} t \\ b \end{pmatrix}}_L H^\dagger t^c_R + Y'\overline{\begin{pmatrix} q_{5/3} \\ t' \end{pmatrix}}_L H t^c_R + Y''\overline{\begin{pmatrix} q_{5/3} \\ t' \end{pmatrix}}_{L/R} H t''_{R/L} + \tilde{Y}\overline{\begin{pmatrix} t \\ b \end{pmatrix}}_L H^\dagger t''_R$$

$$+ \; Y_b\overline{\begin{pmatrix} t \\ b \end{pmatrix}}_L H b^c_R + m\; \bar{t}''_L t^c_R + m'\overline{\begin{pmatrix} q_{5/3} \\ t' \end{pmatrix}}_L \begin{pmatrix} q_{5/3} \\ t' \end{pmatrix}_R + m''\; \bar{t}''_L t''_R + \text{H.c.} \tag{1}$$

where H represents the SM Higgs doublet and L/R the fermion chiralities. By construction, the vector-like quarks possess same quantum numbers and gauge group representations for the left-handed and right-handed states. We have not written the Yukawa couplings for the first two quark generations as their mixings with the top-partners t', t'' are negligible compared to the t-t'-t'' mixing and the CKM mixing angles are typically small, so that the first two quark generations are decoupled from b, t, t', t''. Note that a field redefinition rotating t^c_R and t''_R can allow to eliminate the m term without loss of generality. A last remark is that the Y'' term could be split in two terms with different chiralities and coupling constants. The Lagrangian (1) gives rise, after EWSB, to this top mass matrix:

$$\mathcal{L}_{\text{mass}} = \overline{\begin{pmatrix} t \\ t' \\ t'' \end{pmatrix}}_L \begin{pmatrix} Yv & 0 & \tilde{Y}v \\ Y'v & m' & Y''v \\ m & Y''v & m'' \end{pmatrix} \begin{pmatrix} t^c \\ t' \\ t'' \end{pmatrix}_R + \text{H.c.} \tag{2}$$

with $v \simeq 174$ GeV the SM vacuum expectation value of the Higgs boson. In our notations of Eq.(2), the parameters Y, Y', Y'' and $\tilde{Y}$ contain the whole sign (i.e. the combination of the $\mathrm{SU(2)_L}$ contraction signs and Yukawa coupling constant signs). Note that vector-like fermions do not require EWSB to acquire mass. The non-trivial consequence of the present t', t'' charge assignment choice is the presence of Yukawa terms in the block diagonal matrix of Eq.(2) associated to the top-partners [99] (such Yukawa matrix elements would be absent in the first case of a unique top-partner). This feature of the mass structure allows strong suppressions of the gluon fusion mechanism. In particular, the own top-partner (t', t'') Yukawa coupling (Y'') sign can be chosen independently of the top (t) Yukawa coupling (Y) sign in order to generate destructive interferences between the top and top-partner loops.

III. t_2 RATES AND DIRECT CONSTRAINTS

We consider here the model described in the previous section, where t', t'' denote the states in the interaction basis while t_1, t_2, and t_3 stand for the mass eigenstates, with $m_{t_3} > m_{t_2} > m_{t_1}$, t_1 being the standard top quark and m_{t_1} its physical mass. We concentrate on the phenomenology of the lighter top eigenstate t_2; the t_3 eigenstate production is sub-dominant given its higher mass. In a second stage, one should add the contributions to the Higgs production from the t_3 decays like $t_3 \to t_1 h$ or $t_3 \to t_2 Z$.

In Table I, we define our benchmark points by the values of the fundamental parameters – including the Higgs mass m_h – and the corresponding m_{t_2}, m_{t_3} values. These sets of parameters are selected in particular to have a large branching fraction $B_{t_2 \to t_1 h}$ increasing the studied Higgs signal. Note that in the minimal model with a unique doublet $(q_{5/3}, t')$, $B_{t_2 \to bW}$ is negligible compared to $B_{t_2 \to t_1 h}$ and $B_{t_2 \to t_1 Z}$ [42]. For none of the considered benchmark points, the channel $t_2 \to q_{5/3} W$ is open. Table I also provides the theoretical t_2 widths and the $\sigma_{\bar{t}_2 t_2}$ cross sections for the t_2 pair production at LHC computed with the HATHOR program [70] at NNLO. As a comparison, we give also in able I the expected SM cross sections [71] for Higgs production via gluon fusion, $\sigma^{\text{SM}}_{\text{gg}\to\text{h}}$. It is physically important to note that the branching ratios $B_{t_2 \to t_1 h}$ and $B_{t_2 \to t_1 Z}$ are not vanishing in contrast with the case of a fourth generation t' quark so that the observation of such decays (discussed in Section VI) would even prove the vector-like nature of a heavy top-like quark.

Table I presents finally the CMS constraints on the observables $\sigma_{\bar{t}_2 t_2} B^2_{t_2}$ derived from the search for pair production of a heavy top-like quark [72, 73] (present bounds from ATLAS are less stringent [74]). It appears that the corresponding theoretical values, predicted in the models considered here, respect those experimental limits for m_{t_2} as low as ~ 400 GeV [100]. Increasing theoretically $B_{t_2 \to t_1 h}$, and consequently lowering $B_{t_2 \to t_1 Z}$ and $B_{t_2 \to bW}$, is allowed within these constraints.

Due to these lower limits on m_{t_2} typically around 400 GeV, the t_2 pair production suffers from a significant phase space suppression so that the rate for a single Higgs production through the t_2 decay is smaller than for the standard gluon fusion mechanism; there is *e.g.* a factor of ~ 10 for point A1 at 14 TeV, as shown the Table I. However, the number of Higgs events issued from the t_2 decay can be significant at 14 TeV with suitable luminosities. This Higgs production channel can thus be an interesting Higgs, and t_2, discovery channel, among others, in cases where the gluon fusion mechanism is suppressed by the presence of t', t'' states, as it occurs for instance in point B (see Table I).

Parameter Set	A1	A2	B	C	D
Y / $\tilde{Y}$	-1.43 / 2	1.02 / -0.1	1.15 / 0.4	1.12 / -0.5	1.05 / -0.3
Y' / Y''	1.85 / -1	1 / 0.55	-1.5 / 1.6	1.1 / 1.65	1.7 / 1.9
m / m' (GeV)	0 / 370	0 / 675	0 / 770	0 / 810	80 / 1100
m'' (GeV)	510	645	980	850	1100
m_{t_3} (GeV)	722	804	1181	1125	1454
m_{t_2} (GeV)	403	599	626	572	788
m_h (GeV)	125	125	255	320	540
$\sigma^{\rm SM}_{\rm gg\to h}$ (pb) @ 7 TeV	15.31	15.31	3.18	2.25	0.58
$\sigma^{\rm SM}_{\rm gg\to h}$ (pb) @ 14 TeV	49.85	49.85	13.50	10.59	3.85
$\sigma^{\rm t'}_{\rm gg\to h}/\sigma^{\rm SM}_{\rm gg\to h}$	1.27	1.31	0.45	0.40	0.65
$\sigma^{t'}_{\bar{t}_1 t_1 h}$ (pb) @ 7 TeV	0.0194	0.076	0.0037	0.0016	$7\ 10^{-4}$
$\sigma^{t'}_{\bar{t}_1 t_1 h}$ (pb) @ 14 TeV	0.138	0.0539	0.036	0.021	0.015
$\sigma_{\bar{t}_2 t_2}$ (pb) @ 7 TeV	1.361	0.0936	0.0709	0.136	0.0115
$\sigma_{\bar{t}_2 t_2}$ (pb) @ 14 TeV	13.53	1.465	1.164	1.975	0.284
$B_{t_2\to t_1 h}$ (%)	62.6	82.1	60.8	13.5	43.0
$B_{t_2\to t_1 Z}$ (%)	28.6	14.7	25.0	46.1	40.3
$B_{t_2\to bW}$ (%)	8.8	3.2	14.2	40.4	16.6
Γ_{t_2} (GeV)	4.4	3.5	19.8	6.5	8.8
$\sigma_{\bar{t}_2 t_2} B^2_{t_2\to bW}$ (pb)	0.01	$8\ 10^{-5}$	0.001	0.022	0.000(3)
LHC bound [72]	< 0.26	< 0.14	< 0.14	< 0.16	×
$\sigma_{\bar{t}_2 t_2} B^2_{t_2\to t_1 Z}$ (pb)	0.11	0.002	0.004	0.029	0.002
LHC bound [73]	< 0.5	< 0.4	< 0.4	< 0.4	×
S / T	0.05 / 0.05	0.03 / 0.03	-0.01 / 0.23	-0.01 / 0.30	-0.01 / 0.28

TABLE I: Benchmark scenario in the present t', t'' model, defined by the values of the fundamental parameters, including the Higgs mass, m_h, and the resulting m_{t_2} and m_{t_3} physical masses of the heavy top-like quarks. The cross sections at NNLO, $\sigma_{\bar{t}_2 t_2}$, for the $pp \to t_2\bar{t}_2$ process, are shown at $\sqrt{s} = 7$ TeV or 14 TeV, together with the t_2 widths Γ_{t_2} and the t_2 branching fraction values. For comparison, the SM Higgs production cross-section values via gluon fusion are also given, together with the ratio $\sigma^{\rm t'}_{\rm gg\to h}/\sigma^{\rm SM}_{\rm gg\to h}$, between the gluon fusion cross-section in the present model and the corresponding SM cross-section. Furthermore, the NLO cross-sections for Higgs production in association with a $t\bar{t}$ pair, $\sigma^{t'}_{\bar{t}_1 t_1 h}$, in the present model, are shown in comparison with the $\sigma_{\bar{t}_2 t_2}$ cross-sections. Finally, the LHC upper limits and theoretical predictions for the observables $\sigma_{\bar{t}_2 t_2} B^2_{t_2\to bW}$, $\sigma_{\bar{t}_2 t_2} B^2_{t_2\to t_1 Z}$ are shown just above the last line (the crosses indicate the absence of experimental limit at the associated m_{t_2} values). In the last line are the values of the oblique parameters S and T are given [after subtraction of the SM contributions so that those only include new physics effects]. For the point A1 (A2), we have used the indicated Y'' value for the t''_R coupling and $Y'' = -0.3$ (-1.75) for the t''_L vertex.

IV. CONSTRAINTS FROM THE DIRECT HIGGS BOSON SEARCH

Sets **A1/A2** - At $m_h = 125$ GeV, all the sensitive channels for searching the Higgs boson at hadron colliders are the decays $h \to \gamma\gamma$, $h \to WW$ (with $W \to \ell\nu$), $h \to ZZ$ (with $Z \to \ell\bar{\ell}$), $h \to \tau\bar{\tau}$ and $h \to b\bar{b}$. The latest bounds on the Higgs boson rates obtained at the LHC read as, $\sigma_{\rm gg\to h} B_{\rm h\to\gamma\gamma}/\sigma^{\rm SM}_{\rm gg\to h} B^{\rm SM}_{\rm h\to\gamma\gamma} \lesssim 2$, $\sigma_{\rm gg\to h} B_{\rm h\to WW}/\sigma^{\rm SM}_{\rm gg\to h} B^{\rm SM}_{\rm h\to WW} \lesssim 1.30$, $\sigma_{\rm gg\to h} B_{\rm h\to ZZ}/\sigma^{\rm SM}_{\rm gg\to h} B^{\rm SM}_{\rm h\to ZZ} \lesssim 2.2$, $\sigma_{\rm gg\to h} B_{\rm h\to\tau\tau}/\ \sigma^{\rm SM}_{\rm gg\to h} B^{\rm SM}_{\rm h\to\tau\tau} \lesssim 3.2$ and $\sigma_{\rm gg\to h} B_{\rm h\to bb}/\sigma^{\rm SM}_{\rm gg\to h} B^{\rm SM}_{\rm h\to bb} \lesssim 3.2$ [66–69, 75, 76]. These bounds are compatible with the rates calculated taking into account the $t - t' - t''$ mixing effect on the top quark Yukawa coupling as well as the t_2 and t_3 eigenstate contributions in the triangular loop of the gluon fusion mechanism, for our parameter sets A1/A2. This parameter set yields indeed:

$$\sigma^{\rm t'}_{\rm gg\to h} B^{\rm t'}_{\rm h\to\gamma\gamma}/\sigma^{\rm SM}_{\rm gg\to h} B^{\rm SM}_{\rm h\to\gamma\gamma} = 1.16\ (1.19)\ \ ;\ \ \sigma^{\rm t'}_{\rm gg\to h} B^{\rm t'}_{\rm h\to WW}/\sigma^{\rm SM}_{\rm gg\to h} B^{\rm SM}_{\rm h\to WW} = 1.25\ (1.28) \tag{3}$$

$$\sigma^{\rm t'}_{\rm gg\to h} B^{\rm t'}_{\rm h\to ZZ}/\sigma^{\rm SM}_{\rm gg\to h} B^{\rm SM}_{\rm h\to ZZ} = 1.25\ (1.28)\ \ ;\ \ \sigma^{\rm t'}_{\rm gg\to h} B^{\rm t'}_{\rm h\to\tau\tau}/\sigma^{\rm SM}_{\rm gg\to h} B^{\rm SM}_{\rm h\to\tau\tau} = 1.25\ (1.28) \tag{4}$$

$$\sigma^{\rm t'}_{\rm gg\to h} B^{\rm t'}_{\rm h\to bb}/\sigma^{\rm SM}_{\rm gg\to h} B^{\rm SM}_{\rm h\to bb} = 1.25\ (1.28) \quad [A1]\ ([A2]) \tag{5}$$

The cross section for the Higgs production is enhanced,

$$\sigma^{\rm t'}_{\rm gg\to h}/\sigma^{\rm SM}_{\rm gg\to h} = 1.27\ [A1]\ (1.31\ [A2]),$$

due to the combination of two possible effects: the increase of the t_1 Yukawa coupling and the constructive interferences between the t_1 contribution and the t_2, t_3 ones. In contrast, the branching fraction for the decay channel into diphoton is slightly decreased,

$$B^{\rm t'}_{\rm h\to\gamma\gamma}/B^{\rm SM}_{\rm h\to\gamma\gamma} = 0.91\ [A1]\ (0.90\ [A2]).$$

But the resulting product $\sigma^{\rm t'}_{\rm gg\to h}B^{\rm t'}_{\rm h\to\gamma\gamma}$ is increased relatively to the SM case as shown in Eq.(3).
Such an increased value of the observable $\sigma_{\rm gg\to h}B_{\rm h\to\gamma\gamma}$, induced here by the presence of t' quarks (*c.f.* Eq.(3)), could be indicated by the slight excess in the ATLAS [67, 68, 75, 76] and CMS [66, 69, 75] data corresponding to a possible ∼125 GeV Higgs signal in the diphoton channel. All the values of the quantities, $\sigma^{\rm t'}_{\rm gg\to h}B^{\rm t'}_{\rm h\to\gamma\gamma}/\sigma^{\rm SM}_{\rm gg\to h}B^{\rm SM}_{\rm h\to\gamma\gamma}$, $\sigma^{\rm t'}_{\rm gg\to h}B^{\rm t'}_{\rm h\to WW}/\sigma^{\rm SM}_{\rm gg\to h}B^{\rm SM}_{\rm h\to WW}$, $\sigma^{\rm t'}_{\rm gg\to h}B^{\rm t'}_{\rm h\to ZZ}/\sigma^{\rm SM}_{\rm gg\to h}B^{\rm SM}_{\rm h\to ZZ}$, $\sigma^{\rm t'}_{\rm gg\to h}B^{\rm t'}_{\rm h\to\tau\tau}/\sigma^{\rm SM}_{\rm gg\to h}B^{\rm SM}_{\rm h\to\tau\tau}$ and $\sigma^{\rm t'}_{\rm gg\to h}B^{\rm t'}_{\rm h\to bb}/\sigma^{\rm SM}_{\rm gg\to h}B^{\rm SM}_{\rm h\to bb}$, in Eq.(3)-(5), are also compatible with the CMS and ATLAS best-fit σ/σ_{SM} values, from the combination of all search channels, of $1.22^{+0.31}_{-0.39}$ [69] (for a Higgs mass hypothesis of 124 GeV) and $0.90^{+0.40}_{-0.37}$ [76] (for a Higgs mass hypothesis of 126 GeV), respectively.
It is also interesting to note that the present theoretical model allows for either an increase of $\sigma^{\rm t'}_{\rm gg\to h}$ compared to the SM, as here for A1/A2, or a decrease as with the parameter sets described in the following.
Sets **B,C** - For these sets of parameters where $m_h = 255$ GeV or 320 GeV, all the Higgs decays have negligible widths relatively to the dominant channels $h \to ZZ$ and $h \to WW$, as in the SM case. Hence the branching fractions $B_{\rm h\to ZZ}$ and $B_{\rm h\to WW}$ remain unchanged in the present model with vector-like top quarks where only the decay widths for $h \to gg$, $h \to \gamma\gamma$ and $h \to \gamma Z$ are modified. In consequence, the experimental limits on $\sigma_{\rm gg\to h}/\sigma^{\rm SM}_{\rm gg\to h} < 0.50$ (0.40) [for $m_h \simeq 255$ (320) GeV] issued from the LHC combined investigations using the $h \to ZZ, WW$ channels exclusively [66–69, 75, 76] can be applied directly to our framework where one gets

$$\sigma^{\rm t'}_{\rm gg\to h}/\sigma^{\rm SM}_{\rm gg\to h} = 0.45\ \ [B]\ \ ;\ \ 0.40\ \ [C] \tag{6}$$

which does not conflict with the above LHC limits.
Note that for the point C, $\sigma^{\rm t'}_{\rm gg\to h}$ is strongly reduced compared to SM. A factor 1/10 could even be achieved in the present theoretical model but variants of the multiplet choice (non-minimal in term of field content), allowing coupling correction cancellations, should then be used instead to pass the indirect constraints discussed in Section V.
Set **D** - For $m_h = 540$ GeV, the Higgs boson is searched only through its decays into ZZ and WW. The strongest bounds on the Higgs rates from the LHC read as $\sigma_{\rm gg\to h}B_{\rm h\to ZZ}/\sigma^{\rm SM}_{\rm gg\to h}B^{\rm SM}_{\rm h\to ZZ} \lesssim 0.90$ and $\sigma_{\rm gg\to h}B_{\rm h\to WW}/\sigma^{\rm SM}_{\rm gg\to h}B^{\rm SM}_{\rm h\to WW} \lesssim 1.45$ [66–69, 75, 76]. These upper limits are clearly in good agreement with the rates calculated in the presence of the t' and t'' states (that modifies $B_{\rm h\to t\bar{t}}$) for the set D, namely,

$$\sigma^{\rm t'}_{\rm gg\to h}B^{\rm t'}_{\rm h\to ZZ}/\sigma^{\rm SM}_{\rm gg\to h}B^{\rm SM}_{\rm h\to ZZ} = 0.69 \qquad \sigma^{\rm t'}_{\rm gg\to h}B^{\rm t'}_{\rm h\to WW}/\sigma^{\rm SM}_{\rm gg\to h}B^{\rm SM}_{\rm h\to WW} = 0.69 \tag{7}$$

where

$$B^{\rm t'}_{\rm h\to ZZ}/B^{\rm SM}_{\rm h\to ZZ} = 1.06 \qquad B^{\rm t'}_{\rm h\to WW}/B^{\rm SM}_{\rm h\to WW} = 1.06\ \ [D].$$

V. THE INDIRECT CONSTRAINTS AND OBLIQUE PARAMETERS

Given the absence of precise measurement for the $Zt\bar{t}$ vertex (coupling directly modified by the $t - t' - t''$ mixing), the main indirect constraints to the present model come from the corrections to the gauge boson vacuum polarizations induced by the loops of $q_{5/3}$,t',t'' states. The values of the oblique parameters S, T that we obtain, according to the preliminary calculations of Ref. [77, 78], are given in Table I. They appear to belong to the 1σ regions induced by the long list of EW precision observables measured mainly at the LEP collider [79].
Remark that the input parameters of Table I (i.e. the theoretical values in the first four lines) have been chosen to fix a panel of characteristic benchmark points for m_{t_2} that pass the indirect constraints as well as the bounds from direct Higgs search described in previous section; however those two types of constraints allow large domains of the parameter space (varying also m_h). The precise setting of the Y coupling reflects mainly the experimental precision on the top quark mass measurement (and not any fine-tuning).

The t', t'' states could contribute to Flavor Changing Neutral Current (FCNC) reactions which are experimentally well constrained; from the theoretical point of view, these FCNC contributions rely precisely on the whole set of Yukawa coupling constants for the entire quark sector. The treatment of such an high degree of freedom in the parameter space is beyond the scope of the present study.

Finally, given the relative heavyness of the t_2 quark, we have checked that the predicted value for the V_{tb} CKM matrix element is in agreement with the experimental measurement close to unity obtained (without assuming 3×3 unitarity) through the single top quark production cross section at Tevatron [79].

VI. HIGGS SIGNAL RECONSTRUCTION IN $t_2\bar{t}_2 \to th + X$ EVENTS

We have studied the sensitivity at the LHC with $\sqrt{s} = 14$ TeV of a search for $pp \to t_2\bar{t}_2$ production, with one of the t_2 decaying to th, and the other decaying to bW or tZ or th, resulting into $thbW$, $thtZ$ and $thth$ final states, respectively. For the signal event generation, we have implemented the couplings of our t_2 model in `FeynRules` [80] [101] interfaced with `MadGRAPH` [81] for the *Monte Carlo* generation, `PYTHIA` [82] for the hadronization part and `DELPHES` [83] for the fast simulation of a typical LHC detector response. Signal events are generated for the t_2 and h masses corresponding to the parameter sets described in Table I, for the three final states $thbW$, $thtZ$ and $thth$. Events corresponding to points A1 and A2 are generated with the Higgs decaying through $h \to \gamma\gamma$, while for points B, C and D the $h \to ZZ$ decay is retained for the sensitivity studies described in this Section. The main backgrounds were generated with `ALPGEN` [84] interfaced to `PYTHIA` and `DELPHES`, as for the signal events. Physics objects used for the analysis (photons, leptons and jets) were defined emulating the requirements used in real CMS Higgs searches in the 2011 data. In particular, we followed closely the physics object definition as for the real data 7 TeV Higgs analysis in the diphoton channel [85] and in the four lepton channel [86].

In the following the quoted number of events and distributions are normalized to an integrated luminosity of 20 fb^{-1} multiplied by, for the different signal final states, their expected $\sigma_{\bar{t}_2 t_2}$ cross-section times branching fractions (hereafter referred to as signal event yield per unit of integrated luminosity), while, for background processes, their `ALPGEN` cross-sections are used. The signal event yield in the different final states depends upon the parameter set under consideration. In Table II, we summarize, for each parameter set described in Table I, the physical signal m_{t_2} and m_h masses, the $\sigma_{\bar{t}_2 t_2}$ cross sections, the t_2 branching fractions into bW ($B_{t_2\to bW}$), tZ ($B_{t_2\to tZ}$), th ($B_{t_2\to th}$) final states, as well as the h branching fractions into $\gamma\gamma$ (for sets A1 and A2) and into ZZ (for sets B, C and D), reporting the expected SM branching fraction values and the factor $f^{t'/SM}_{h\to VV}$ (see Section IV) by which it is modified in the present model. The last three columns of Table II show the expected signal event yield, for $thbW$, $thtZ$ and $thth$ final states, with one Higgs boson decaying via $h \to \gamma\gamma$ or $h \to ZZ$. They are calculated as follows:

$$
\begin{aligned}
&thbW \text{ final state}, \quad Y_S(h \to VV) = \; 2\; B_{t_2\to th} B_{t_2\to bW}\; B^{SM}_{h\to VV} f^{t'/SM}_{h\to VV}\; \sigma_{t_2\bar{t}_2} \\
&thtZ \text{ final state}, \quad Y_S(h \to VV) = \; 2\; B_{t_2\to th} B_{t_2\to tZ}\; B^{SM}_{h\to VV} f^{t'/SM}_{h\to VV}\; \sigma_{t_2\bar{t}_2} \\
&thth \text{ final state}, \quad Y_S(h \to VV) = \; 2\; B^2_{t_2\to th}\; B^{SM}_{h\to VV} f^{t'/SM}_{h\to VV}\; \sigma_{t_2\bar{t}_2}
\end{aligned}
$$

For $thth$ events, the event yield is given for events where one h decays to vector bosons, while the second h decays inclusively. The signal event yield (in fb) multiplied by the integrated luminosity (in fb^{-1}) results into the numbers of produced signal events for that luminosity. We note that, for a chosen Higgs decay, the signal yield depends on both $\sigma_{\bar{t}_2 t_2}$ and $B_{t_2\to th}$. Then, for example, in spite of the fact that $\sigma_{\bar{t}_2 t_2}$ is larger for point C than B, the signal event yield is higher for point B than C, because of the larger $B_{t_2\to th}$ value in point C. The background cross sections are listed in Tablel III, for the four lepton search channel, and in Table IV for the diphoton search channel.

Parameter set	m_{t_2}(GeV)	m_h(GeV)	$\sigma_{\bar{t}_2 t_2}$(fb)	$B_{t_2\to th}$	$B_{t_2\to tZ}$	$B_{t_2\to bW}$	$B^{SM}_{h\to VV}$	$f^{t'/SM}_{h\to VV}$	$Y_S(h\to VV)$(fb)		
									$thbW$	$thtZ$	$thth$
Point A1	403	125	1.353 10^4	0.626	0.286	0.088	2.29 10^{-3}	0.91	3.11	10.1	22.1
Point A2	599	125	1.465 10^3	0.821	0.147	0.032	2.29 10^{-3}	0.90	0.159	0.729	4.07
Point B	626	255	1.164 10^3	0.608	0.25	0.142	0.298	1.00	59.9	105	256
Point C	572	320	1.975 10^3	0.135	0.461	0.404	0.309	1.00	66.6	76.0	22.2
Point D	788	540	0.284 10^3	0.43	0.403	0.166	0.265	1.06	11.4	27.6	29.5

TABLE II: Signal t_2 and h masses, t_2 pair production cross-section at 14 TeV, t_2 branching fractions and event yield Y_S, per unit of integrated luminosity, for the different final states $t_2\bar{t}_2 \to thbW$, $thtZ$, $thth$ and $h \to \gamma\gamma$, for points A1 and A2, or $h \to ZZ$, for point B, C, D. For $thth$ events, the event yield is calculated for the case where one h decays to vector bosons, while the second h decays inclusively.

A. Search for $t_2\bar{t}_2 \to th + X$ signal in the four leptons plus multijets channel

In order to estimate the sensitivity of a search for $thbW$, $thtZ$ and $thth$ final states, when the Higgs boson is relatively heavy, as expected for the points B, C and D, with $m_h = 225, 320, 540$ GeV, respectively, we exploit the decay channel into four charged leptons $h \to ZZ \to 4l$. Signals from $thbW$, $thtZ$, $thth$, $h \to ZZ \to 4l$, final states are characterized by four high transverse momentum leptons, from the Higgs decay, and a large number of energetic jets, from accompanying top and heavy vector boson decays.

The event selection, exploiting the large number of high p_T leptons and jets, as well as the b-jet content of the event, consists of the following criteria:

- Four leptons (muons or electrons) are required with $p_T > 20$ GeV and $|\eta|$ <2.4 or 2.5 for muons or electrons, respectively, and two lepton pairs, each pair with same flavor and opposite charge leptons. The lepton pair of highest p_T is required to have a dilepton mass consistent with the Z mass, $M_{2l} = M_Z \pm 15$ GeV, while the lepton pair with second highest dilepton p_T must have a dilepton mass $M_{2l} > 12$ GeV;
- $H_T > 1000$ GeV and $N_j > 5$, with H_T being defined as the scalar sum of the transverse momenta of identified leptons, photons, jets, and the missing energy, and N_j being the number of hadronic jets with p_T >30 GeV and $|\eta|$ <2.4;
- At least two b-tagged jets in the event.

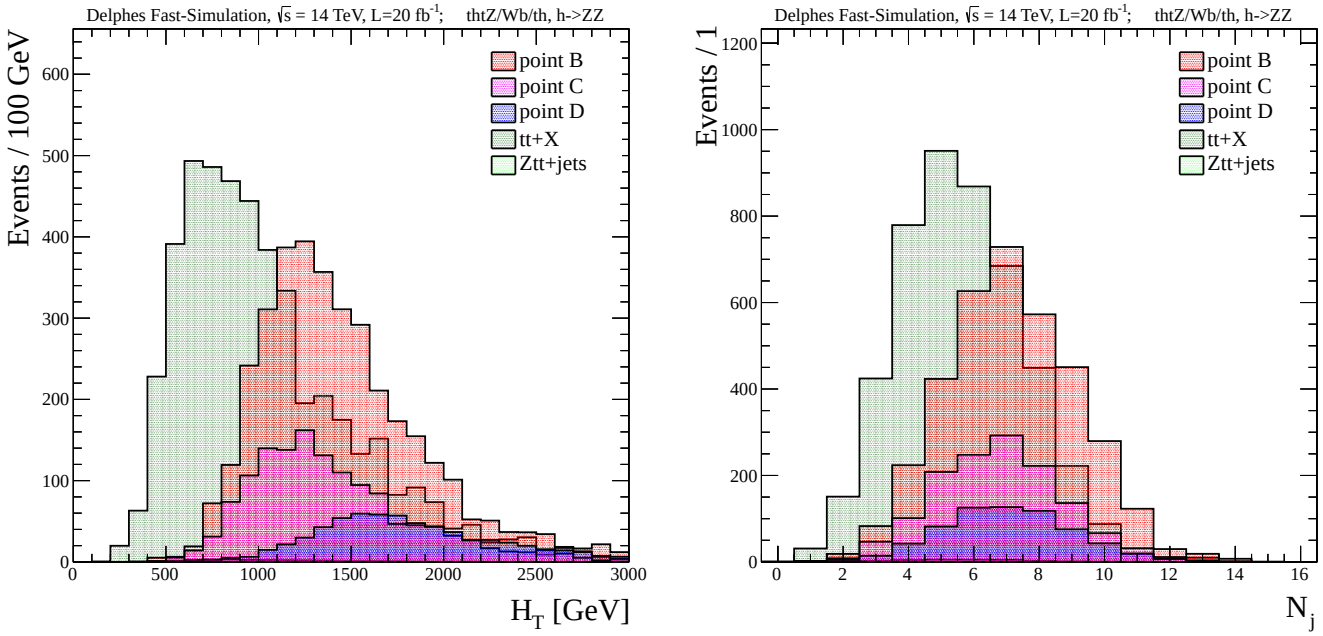

FIG. 1: Distributions of the H_T variable and the jet multiplicity N_j after four lepton requirements. Background and signal distributions are shown overlaid, to compare the different distribution shapes, with the background normalized to the expected events for 20 fb^{-1} and the corresponding signal expectation multiplied by a factor of fifty.

The motivation for the H_T and N_j cuts is evident from Figure 1, showing the H_T and N_j distributions after the four lepton requirements. The event numbers are shown for an integrated luminosity $L = 20$ fb^{-1}, with the signal event numbers multiplied by a factor of fifty, for shape comparison. Expectations for the signals, by final state, and the backgrounds processes, after the selection cuts, for an integrated luminosity of $L = 20$ fb^{-1}, are shown in Table III, where the following quantities are reported:

- Y_S, the signal event number produced, per unit of integrated luminosity, given for each signal parameter set and final state under study, as reported in Table II;
- σ, the cross sections, as calculated by the ALPGEN generator, for the background processes included in the present study;
- N_{4l}, the number of events after four lepton requirements;
- N_{N_j,H_T}, the number of events after the additional requirements $H_T > 1000$ GeV and $N_j > 5$;
- N_{2b}, the number of events after the additional requirements of two b-tagged jets in the event;
- S and B, the total number of signal (summed over all signal final states) and background (summed over all background processes), after a cut on the reconstructed four lepton mass, M_{4l}, with ΔB being the expected statistical uncertainty (standard deviation) on the total number of background events, so that an estimation of the signal sensitivity can then be evaluated as the ratio $S/\Delta B$, measuring the signal in terms of background standard deviations.

	Signal: $thbW/thtZ/thth$, $h \to ZZ$				Total signal S, M_{4l}(GeV) cut			
Parameter set	Y_S (fb)	N_{4l}	N_{N_j,H_T}	N_{2b}	no mass cut	> 200	> 300	> 500
Point B	59.9 / 105 / 256	8.1 / 23.7 / 37.8	5.5 / 18.0 / 28.9	3.52 / 11.5 / 18.5	33.4	30.4	17.0	4.9
Point C	66.6 / 76.0 / 22.2	7.7 / 15.8 / 3.1	4.8 / 11.3 / 2.2	3.07 /7.23 / 1.41	11.7	10.7	7.4	2.0
Point D	11.4 / 27.6 / 29.5	1.5 / 6.6 / 4.7	1.1 / 5.3 / 3.9	0.70 / 3.40 / 2.50	6.6	6.2	5.1	2.7
	Background				Total background B, M_{4l}(GeV) cut			
Process	σ(fb)	N_{4l}	N_{N_j,H_T}	N_{2b}	no mass cut	> 200	> 300	> 500
$t\bar{t}$ + jets	9.19 10^5	4680	1480	27.5	35.5	23.5	13.2	6.8
$t\bar{t}b\bar{b}$ + jets	2.50 10^3	5.60	3.10	2.0	Statistical ΔB, M_{4l}(GeV) cut			
$t\bar{t}W$ + jets	1.99 10^2	1.20	0.40	0.036	no mass cut	> 200	> 300	> 500
$t\bar{t}Z$ + jets	97.3	25.0	9.5	6.0	6.0	4.9	3.6	2.6

TABLE III: Search for $thbW$, $thtZ$ and $thth$ final states, with $h \to ZZ$, in events with four leptons plus multijets, at the 14 TeV LHC: number of events, after different cuts, and final signal significance.

The need for additional cuts, after the leptons, jets and H_T requirements, is seen in Table III, where the N_{N_j,H_T} column shows that after these cuts, a large background, predominantly from $t\bar{t}$ + jets production, is still present. Further background rejection can be obtained with requirements on the number of b-tagged jets. The motivation is the following: in $t\bar{t}$ events the requirement of four high p_T leptons strongly reduces the number of b-taggable jets. Indeed, in $t\bar{t}$+jets events, while two high p_T leptons are provided by the two leptonic W decay, the additional two leptons are preferentially resulting from the two b decays. Thus, applying a b-tagging requirement can reduce significantly the $t\bar{t}$ contribution. In the signal case, the four leptons come mainly from the $h \to ZZ \to 4l$ decay so that there are in average at least two b-taggable jets in the event, for which a b-tagging requirement can have high efficiency. Since no detailed b-tagging information is presently available in `DELPHES`, we make use of known b-tagging and mis-tagging efficiency values as measured by LHC experiments (see *e.g.* Ref. [87]), to estimate the effect on background and signal of requiring two b-tagged jets in the event. The probability for a b-jet to be b-tagged is taken to be $\epsilon_{b-tag} = 0.8$ for a mis-tagging probability is $\epsilon_{b-tag} = 0.05$. An event-by-event weight, that is an estimation of the probability that two b-jets be identified in the event, is applied to both background and signal events.

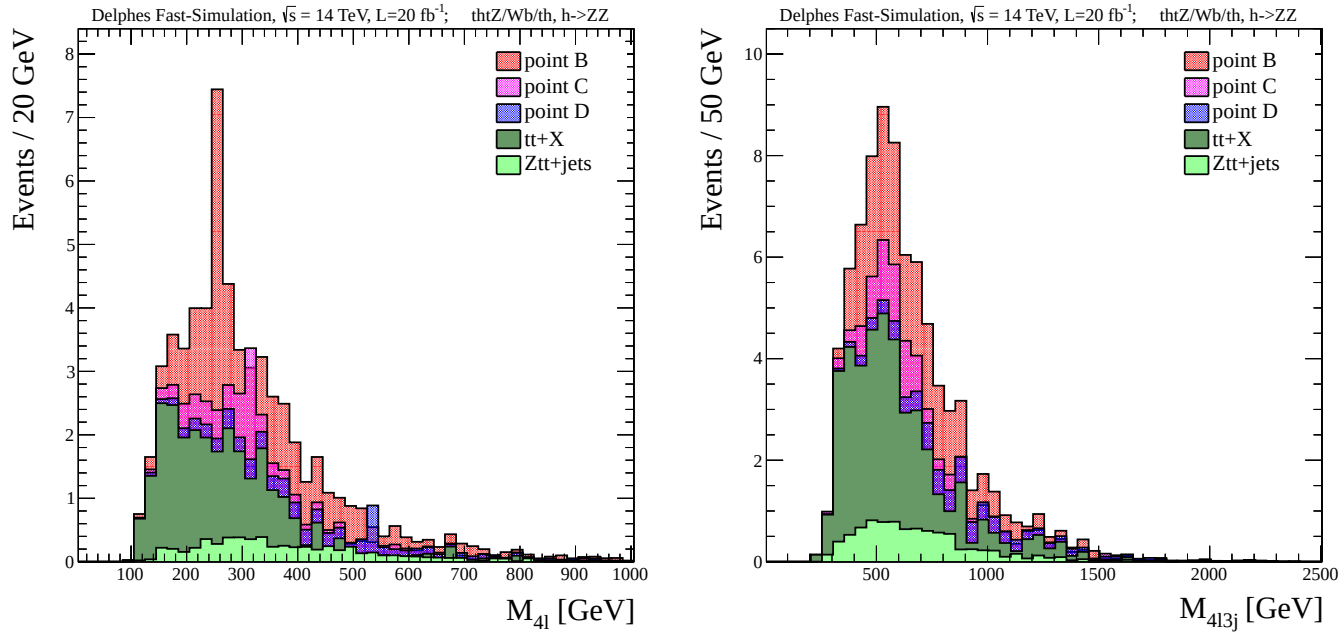

FIG. 2: Distributions of the four lepton mass, M_{4l}, and of the reconstructed heavy mass, M_{4l3j}, after all selection cuts. Signal and background distributions, normalized to the expected events for 20 fb^{-1}, are shown stacked to indicate the relative contributions.

The number of expected events, for signals and backgrounds, resulting from leptons, jets and b-tagging requirement are shown in the column N_{2b} of Table III. The corresponding distributions of the invariant mass of the four leptons, M_{4l}, for signals and backgrounds are shown in Figure 2. The mass peak corresponding to the generated Higgs mass is reconstructed at the correct mass value with good resolution ($\Delta M_{4l}/M_{4l} \lesssim 10\%$). Signal events, with reconstructed mass significantly lower, or higher, than the generated Higgs mass value, are in general events where one lepton from

the $h \to ZZ \to 4l$ decay does not pass the lepton selection criteria, while another lepton from an accompanying W or Z decays is selected to reconstruct the four lepton mass. The background, mainly from the $t\bar{t}$ + jets process, is mostly concentrated in the M_{4l} region below 200 GeV. Applying a lower cut on M_{4l} removes a large fraction of the background and improves the signal significance, as shown in Table III. An additional distribution of the variable, M_{4l3j}, is shown after all but the M_{4l} cuts. This variable can help estimating directly the mass of the heavy top-like quark. It is defined as the invariant mass of the system obtained by associating to the four lepton momentum direction the four closest jets in ΔR. The distributions of M_{4l3j} for signals and backgrounds are shown in Figure 2. A broad peak is observed at about the generated t_2 masses. However, a significantly larger luminosity than for the early discovery is needed to estimate the t_2 mass from these distributions.

The numbers of signal and background events expected after all cuts, and for M_{4l} >200, 300 and 500 GeV, are shown in the three rightmost columns of Table III together with the expected statistical background standard deviation ΔB for the three signal points investigated in this search channel. We estimate that, for an integrated luminosity of 20 fb^{-1}, a signal corresponding to point B is detectable with a significance $S/\Delta B \sim 6$ (after M_{4l} >200 GeV cut). For this benchmark point the $B_{t_2 \to th}$ branching fraction is ~ 0.6. Then, for similar t_2 cross-section, t_2 mass and h mass values, a signal could be discovered, with $S/\Delta B \gtrsim 5$, for $B_{t_2 \to th} \gtrsim 0.5$. For point C, with $B_{t_2 \to th} \sim 0.1$ we obtain a signal significance $S/\Delta B \sim 2$. A signal significance of five and above is then obtained, with $L = 20$ fb^{-1}, for $B_{t_2 \to th} \gtrsim 0.25$. For smaller $B_{t_2 \to th}$ values, a larger integrated luminosity, or a more optimal analysis, would be needed for a signal significance of five or above. For point D, with $B_{t_2 \to th} \sim 0.4$, we obtain a signal significance $S/\Delta B \sim 1.4$ thus even for maximal $B_{t_2 \to th} \sim 1$ a signal significance of ~ 3.5 is attainable. Higher integrated luminosity, or higher background rejection, depending on the $B_{t_2 \to th}$ value (for $B_{t_2 \to th} \sim 0.4$, about a factor of ten larger luminosity or background rejection) is needed for a five sigma signal significance corresponding to the D scenario, with a t_2 mass of about 800 GeV and a pair production cross section of about 0.3 pb.

B. Search for $t_2\bar{t_2} \to th + X$ signal in the diphoton plus multi-jet channel

To study the sensitivity of a search for $thtZ$, $thbW$ and $thth$ final states, when the Higgs is relatively light, as for points A1 and A2, with $m_h = 125$ GeV, we exploit the $h \to \gamma\gamma$ decay channel. As for a light Higgs in the SM, in spite of the relatively small expected B($h \to \gamma\gamma$) value, this is expected to be a channel with good signal sensitivity, due to the good diphoton mass resolution, allowing to identify the Higgs mass signal over a background that can be well measured in the side-bands.

The background processes considered in this study are listed in Table IV. To reduce generation time for the background events, we have applied cuts on `ALPGEN` generated parton quantities, that are looser than the cuts applied on the reconstructed physics objects. The generator level cuts are: photon $p_T > 20$ GeV and $|\eta|$ <3.0, jet $p_T > 20$ GeV and $|\eta| < 2.5$, $\Delta R_{\gamma j} < 0.4$, $\Delta R_{\gamma l} < 0.4$, , $\Delta R_{jj} < 0.4$ and $\Delta R_{t\bar{t}} < 0.4$. Background cross-sections for these generator level cuts as calculated by `ALPGEN` are listed in Table IV. An additional background is the $\gamma\gamma$+jets process. A relatively large inclusive diphoton cross-section is expected [88] and is going to be measured at the LHC, together with the contribution from fake diphoton pairs. The inclusive diphoton cross section in the diphoton mass region of interest can be large (order of pb), but we expect that the large jet multiplicity requirement scales down this contribution by at least three orders of magnitude, thus reducing its cross-section to few fb. An additional handle to minimize this background will be the b-tagging, that can reduce the contribution from light flavored multi-jets events by two or three order of magnitudes (as discussed in the previous Section), while retaining a large fraction of the signal events containing at least two b-jets. However, b-tagging will not effectively reduce backgrounds with t-quark pairs in the final state, as in the case of $t\bar{t}\gamma\gamma$+ jets process. Thus, conservatively we have not exploited b-tagging for this analysis of the $h \to \gamma\gamma$ channel.

Signals from $thbW$, $thtZ$, $thth$, $h \to \gamma\gamma$, final states are characterized by a large number of energetic jets, from top and heavy vector boson decays, in addition to the two high transverse momentum photons from the Higgs decay. The event selection consists of the following criteria:

- Photons are required to be within $|\eta| < 2.5$ and isolated. The isolation requirements imply that, within a cone $\Delta R = 0.4$ around the photon direction, the charged particle energy measured in the tracker is < 2.0 GeV, the electromagnetic calorimeter (ecal) energy in the cone is < 4.2 GeV, the hadronic calorimeter (hcal) energy in the cone is < 2.2 GeV and the ratio between the ecal and hcal energy in the cone is < 0.05. Two isolated photons are required, with the leading photon $p_T > 45$ GeV and the second photon $p_T > 30$ GeV. The invariant mass of the two photon is required to be $M_{2\gamma} > 90$ GeV.

- Hadronic jets are counted if they have p_T >30 GeV and $|\eta| < 2.4$. Events are required to have a number of jets $N_j > 6$, at preselection, or $N_j > 8$, for the final selection, after which the signal sensitivity is evaluated in a sliding $M_{2\gamma}$ window.

Figure 3, shows the H_T and N_j distributions after the diphoton and $M_{2\gamma} > 90$ GeV requirements. The distributions are shown for an integrated luminosity $L = 20$ fb^{-1}, with the signal expectation for point A2 multiplied by a factor of ten, for shape comparison. Because of the relatively light t_2 mass in point A1, an $H_T > 1000$ GeV cut, as applied for

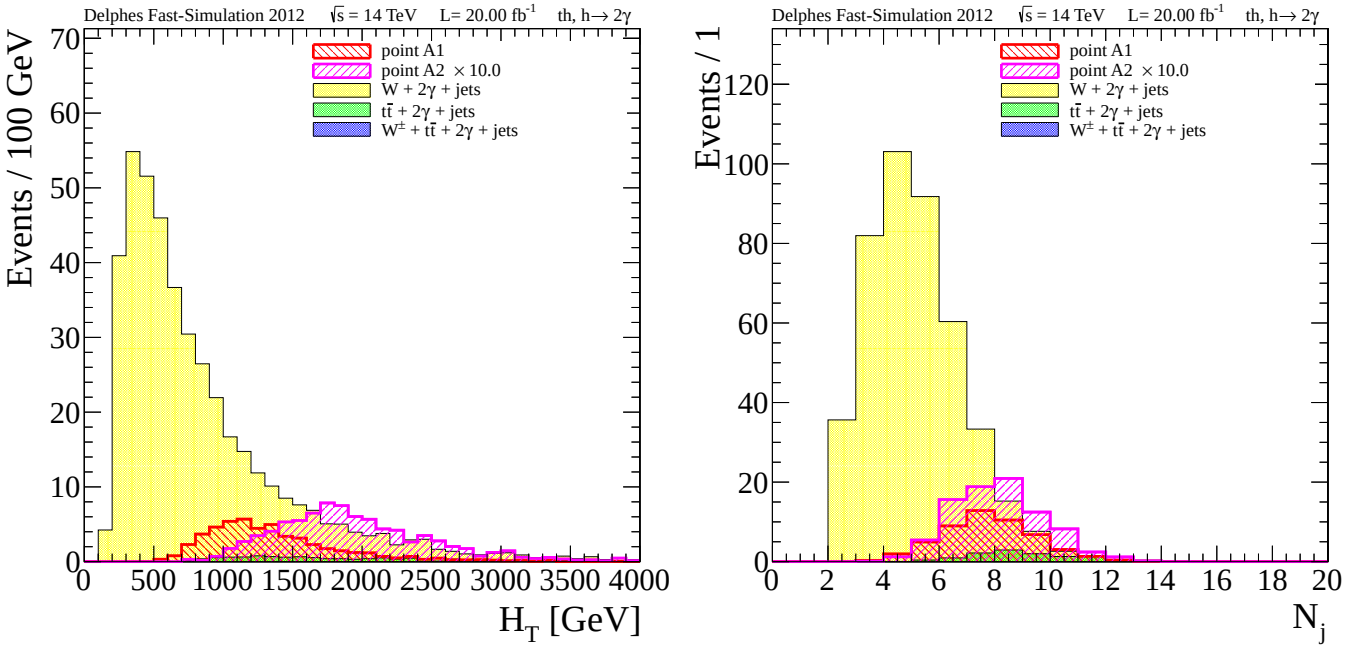

FIG. 3: Distributions of the H_T variable and the jet multiplicity N_j after diphoton and $M_{2\gamma} > 90$ GeV requirements.

points B, C and D, would reject a significant fraction of this signal. A lower H_T cut would not improve significantly the signal-over-background ratio after the N_j requirement, thus no H_T cut is applied in this channel. Expectations for the signals, by final state, and the backgrounds processes, after the selection cuts, for an integrated luminosity of $L = 20$ fb^{-1}, are shown in Table IV, where the following quantities are reported:

- Y_S, the signal event number produced, per unit of integrated luminosity, given for each signal parameter set and final state under study, as reported in Table II;
- σ, the background cross sections, as calculated from the ALPGEN generator, for the background processes included in the present study;
- $N_{2\gamma}$, the number of events after diphoton and $M_{2\gamma} > 90$ GeV requirements;
- $N_{N_j>6}$ and $N_{N_j>8}$ the number of events after the additional jet multiplicity cuts;
- S and B, the total number of signal (summed over all signal final states) and background (summed over all background processes), after a cut $M_{2\gamma}$, with ΔB being the expected statistical uncertainty (standard deviation) on the total number of background events. An estimation of the expected signal sensitivity can then be evaluated as the ratio $S/\Delta B$, measuring the signal in terms of background standard deviations.

	Signal: $thbW/thtZ/thth$, $h \to \gamma\gamma$				Total signal S, $M_{2\gamma}$(GeV) cut	
Parameter set	Y_S (fb)	$N_{2\gamma}$	$N_{N_j>6}$	$N_{N_j>8}$	> 90	[115,135]
Point A1	3.1 / 10.1 / 22.1	5.4 / 15.4 / 30.4	4.1 / 12.7 / 27.1	1.4 / 6.2 / 14.5	22.1	17.7
Point A2	0.16 / 0.73 / 4.1	0.34 / 1.35 / 6.98	0.27 / 1.17 / 6.6	0.10 / 0.62 / 3.8	4.5	3.2
	Background				Tot, background B, $M_{2\gamma}$(GeV) cut	
Process	σ(fb)	$N_{M_{2\gamma}>90}$	$N_{N_j>6}$	$N_{N_j>8}$	> 90	[115,135]
$W\gamma\gamma$ + jets	450	422	110	19.6	27.8	4.38
$t\bar{t}\gamma\gamma$ + jets	15.5	11.8	11.3	8.18	Statistical ΔB, $M_{2\gamma}$(GeV) cut	
$t\bar{t}W\gamma\gamma$ + jets	0.0678	0.0577	0.0515	0.0272	> 90	[115,135]
					5.3	2.1

TABLE IV: Search for $thbW$, $thtZ$ and $thth$ final states, with $h \to \gamma\gamma$, in events with two photons plus multijets, at the 14 TeV LHC: number of events, after different cuts, and final signal significance.

In virtue of the good diphoton mass resolution (∼1% to 5% for a 110 to 130 GeV Higgs, depending on photon selection criteria) of the detector, a highly discriminating quantity after selection is the reconstructed diphoton mass. The diphoton invariant mass distribution for signals and backgrounds events, after the $N_j > 8$ requirement, is shown

in Figure 4. Also shown is the distribution of an additional variable, $M_{re\ nj}$, that could help estimating the mass of the heavy top-like quark. This is defined as the invariant mass of the system of n jets recoiling against the diphoton+m jets system, where the m jets are the closest in ΔR to the diphoton direction. The recoiling n jets, with $n = N_j - m$, are counted to minimize, among all m and n choices in the event, the difference between the mass of the diphoton+m jets system and the mass of the recoiling n jets, The distributions of $M_{re\ nj}$ for signals and backgrounds, after all but the $M_{2\gamma}$ window cut, are shown in Figure 4. A broad peak, whose width is dominated by the jet energy resolution, is observed at about the generated t_2 masses. The t_2 mass can be estimated directly from these distributions, with a relatively large uncertainty and larger luminosity than needed for a five sigma excess observation in the $M_{2\gamma}$ distribution. The total number of signal and background events, after diphoton and jet multiplicity requirements,

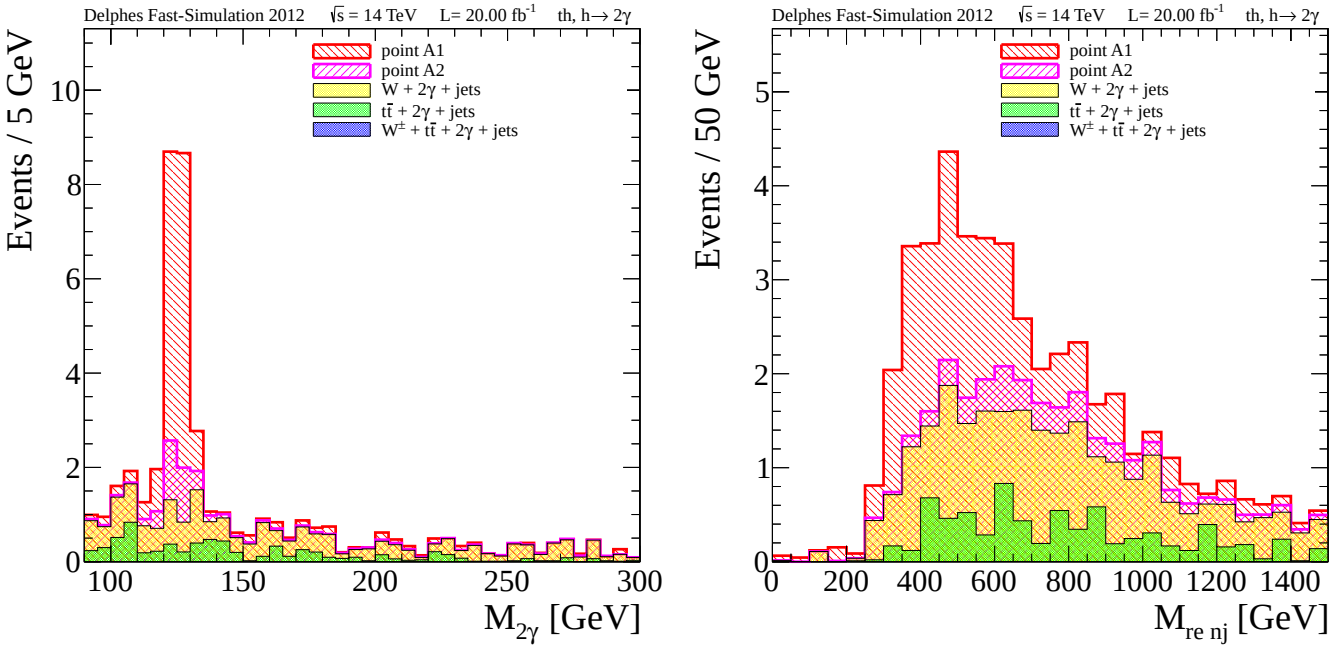

FIG. 4: Distributions of the diphoton mass, $M_{2\gamma}$, and of the reconstructed heavy recoil mass, $M_{re\ nj}$, after all selection cuts.

with a diphoton mass in the window between 115 GeV and 135 GeV, is also given in Table IV. We estimate that for an integrated luminosity of 20 fb^{-1}, a signal, corresponding to the benchmark point A1, is detectable with a significance $S/\Delta B \sim 9$. For this benchmark point the $B_{t_2\to th} \sim 0.6$. Then, for a similar t_2 cross-section and t_2, h mass values, a signal could still be discovered, with a signal significance of about or above five, for if $B_{t_2\to th} \gtrsim 0.3$. For point A2, where the $\sigma_{\bar{t}_2 t_2}$ is about an order of magnitude lower than in point A1, while $B_{t_2\to th} \sim 0.8$, the expected signal significance is ~ 1.5. Then, to reach a signal significance of five, at least a factor of ten larger luminosity, or a better background rejection, is needed to observe this signal.

VII. CONCLUSIONS

We have shown that there exist regions of the parameter space in beyond SM scenarios, allowed by present phenomenological and experimental constraints, in particular by the direct Higgs searches, where heavy vector-like top partner production at the LHC may give rise to new Higgs production channels, over a large Higgs mass range, extending from 120 GeV to more than 500 GeV. Indeed the SM Higgs mass exclusion, in the range between $\sim$ 130 and 600 GeV, does not hold in these beyond SM scenarios. We have shown that for a variety of heavy top and Higgs mass values, and expected heavy top pair production cross sections and decay branching fraction values, a signal of Higgs production, from the decay of a heavy top, could be detectable at the 14 TeV LHC, with an integrated luminosity between $\sim$20 fb^{-1} to $\sim$200 fb^{-1}, over a large Higgs mass range ($\sim$120 GeV to $\sim$600 GeV), exploiting the diphoton and four lepton mass distributions. The Higgs mass peak arising in those distributions can be reconstructed with a good mass resolution ($\sim$ 2-5% for the diphoton channel and $\sim$ 5-10% in the four lepton channel). Finally, we have proposed new mass variables from which the heavy top mass could be directly estimated.

ACKNOWLEDGEMENTS

The work of G.M. is supported by the ANR *CPV-LFV-LHC* under project **NT09-508531** and *TAPDMS* under project **09-JCJC-0146**. D.K.G. acknowledges partial support from the Department of Science and Technology, India under the grant SR/S2/HEP-12/2006.

---

[1] N. Arkani-Hamed, A. G. Cohen, and H. Georgi, Phys. Lett. **B513**, 232 (2001), hep-ph/0105239.
[2] N. Arkani-Hamed et al., JHEP **08**, 021 (2002), hep-ph/0206020.
[3] N. Arkani-Hamed, A. Cohen, E. Katz, and A. Nelson, JHEP **0207**, 034 (2002), hep-ph/0206021.
[4] R. Contino, Y. Nomura, and A. Pomarol, Nucl.Phys. **B671**, 148 (2003), hep-ph/0306259.
[5] K. Agashe, R. Contino, and A. Pomarol, Nucl.Phys. **B719**, 165 (2005), hep-ph/0412089.
[6] K. Agashe and R. Contino, Nucl.Phys. **B742**, 59 (2006), hep-ph/0510164.
[7] R. Contino, L. Da Rold, and A. Pomarol, Phys.Rev. **D75**, 055014 (2007), hep-ph/0612048.
[8] G. Burdman and L. Da Rold, JHEP **0712**, 086 (2007), 0710.0623.
[9] C. T. Hill, Phys.Lett. **B266**, 419 (1991).
[10] H.-C. Cheng, B. A. Dobrescu, and C. T. Hill, Nucl.Phys. **B589**, 249 (2000), hep-ph/9912343.
[11] M. S. Carena, E. Ponton, J. Santiago, and C. E. Wagner, Nucl.Phys. **B759**, 202 (2006), hep-ph/0607106.
[12] M. S. Carena, E. Ponton, J. Santiago, and C. Wagner, Phys.Rev. **D76**, 035006 (2007), hep-ph/0701055.
[13] L. Randall and R. Sundrum, Phys.Rev.Lett. **83**, 3370 (1999), hep-ph/9905221.
[14] M. Gogberashvili, Int.J.Mod.Phys. **D11**, 1635 (2002), hep-ph/9812296.
[15] T. Gherghetta and A. Pomarol, Nucl.Phys. **B586**, 141 (2000), hep-ph/0003129.
[16] K. Agashe, A. Delgado, M. J. May, and R. Sundrum, JHEP **0308**, 050 (2003), hep-ph/0308036.
[17] C. Bouchart and G. Moreau, Nucl.Phys. **B810**, 66 (2009), 0807.4461.
[18] A. Djouadi, G. Moreau, and F. Richard, Nucl.Phys. **B773**, 43 (2007), hep-ph/0610173.
[19] A. Djouadi, G. Moreau, and R. K. Singh, Nucl.Phys. **B797**, 1 (2008), 0706.4191.
[20] K. Agashe, R. Contino, L. Da Rold, and A. Pomarol, Phys.Lett. **B641**, 62 (2006), hep-ph/0605341.
[21] C. Bouchart and G. Moreau, Phys.Rev. **D80**, 095022 (2009), 0909.4812.
[22] C. Kilic, K. Kopp, and T. Okui, Phys.Rev. **D83**, 015006 (2011), 1008.2763.
[23] S. J. Huber and Q. Shafi, Phys.Lett. **B498**, 256 (2001), hep-ph/0010195.
[24] S. J. Huber and Q. Shafi, Phys.Lett. **B512**, 365 (2001), hep-ph/0104293.
[25] S. J. Huber and Q. Shafi, Phys.Lett. **B544**, 295 (2002), hep-ph/0205327.
[26] S. J. Huber and Q. Shafi, Phys.Lett. **B583**, 293 (2004), hep-ph/0309252.
[27] S. Chang, C. Kim, and M. Yamaguchi, Phys.Rev. **D73**, 033002 (2006), hep-ph/0511099.
[28] G. Moreau and J. Silva-Marcos, JHEP **0603**, 090 (2006), hep-ph/0602155.
[29] G. Moreau and J. Silva-Marcos, JHEP **0601**, 048 (2006), hep-ph/0507145.
[30] K. Agashe, G. Perez, and A. Soni, Phys.Rev. **D71**, 016002 (2005), hep-ph/0408134.
[31] K. Agashe, G. Perez, and A. Soni, Phys.Rev.Lett. **93**, 201804 (2004), hep-ph/0406101.
[32] K. Agashe, G. Perez, and A. Soni, Phys.Rev. **D75**, 015002 (2007), hep-ph/0606293.
[33] K. Agashe, A. E. Blechman, and F. Petriello, Phys.Rev. **D74**, 053011 (2006), hep-ph/0606021.
[34] Y. Grossman and M. Neubert, Phys.Lett. **B474**, 361 (2000), hep-ph/9912408.
[35] T. Appelquist, B. A. Dobrescu, E. Ponton, and H.-U. Yee, Phys.Rev. **D65**, 105019 (2002), hep-ph/0201131.
[36] T. Gherghetta, Phys.Rev.Lett. **92**, 161601 (2004), hep-ph/0312392.
[37] G. Moreau, Eur.Phys.J. **C40**, 539 (2005), hep-ph/0407177.
[38] G. Cacciapaglia, A. Deandrea, D. Harada, and Y. Okada, JHEP **1011**, 159 (2010), 1007.2933.
[39] G. Cacciapaglia, A. Deandrea, L. Panizzi, N. Gaur, D. Harada, et al. (2011), 1108.6329.
[40] S. Gopalakrishna, T. Mandal, S. Mitra, and R. Tibrewala, Phys.Rev. **D84**, 055001 (2011), 1107.4306.
[41] J. Aguilar-Saavedra, Phys.Lett. **B625**, 234 (2005), hep-ph/0506187.
[42] J. Aguilar-Saavedra, JHEP **0911**, 030 (2009), 0907.3155.
[43] A. Ivanov (CDF and D0 Collaboration) (2011), 14 pages, 6 figures, FPCP 2011 Conference Proceedings, 1109.1025.
[44] G. Burdman, M. Perelstein, and A. Pierce, Phys.Rev.Lett. **90**, 241802 (2003), hep-ph/0212228.
[45] T. Han, H. E. Logan, B. McElrath, and L.-T. Wang, Phys.Rev. **D67**, 095004 (2003), hep-ph/0301040.
[46] M. Perelstein, M. E. Peskin, and A. Pierce, Phys.Rev. **D69**, 075002 (2004), hep-ph/0310039.
[47] H.-C. Cheng, I. Low, and L.-T. Wang, Phys.Rev. **D74**, 055001 (2006), hep-ph/0510225.
[48] G. Cacciapaglia, S. Choudhury, A. Deandrea, N. Gaur, and M. Klasen, JHEP **1003**, 059 (2010), 0911.4630.
[49] N. Vignaroli (2011), 1107.4558.
[50] R. Contino and G. Servant, JHEP **0806**, 026 (2008), 0801.1679.
[51] C. Dennis, M. Karagoz, G. Servant, and J. Tseng (2007), hep-ph/0701158.
[52] K. Agashe and G. Servant, JCAP **0502**, 002 (2005), hep-ph/0411254.
[53] G. Brooijmans et al. (New Physics Working Group), pp. 191–380 (2010), 1005.1229.
[54] C. Bini, R. Contino, and N. Vignaroli, JHEP **1201**, 157 (2012), 1110.6058.
[55] R. Barcelo, A. Carmona, M. Masip, and J. Santiago, Phys.Lett. **B707**, 88 (2012), 1106.4054.
[56] R. Barcelo, A. Carmona, M. Chala, M. Masip, and J. Santiago, Nucl.Phys. **B857**, 172 (2012), 1110.5914.
[57] F. del Aguila, L. Ametller, G. L. Kane, and J. Vidal, Nucl. Phys. **B334**, 1 (1990).

[58] F. del Aguila, G. L. Kane, and M. Quiros, Phys. Rev. Lett. **63**, 942 (1989).
[59] G. D. Kribs, A. Martin, and T. S. Roy (2010), 1012.2866.
[60] G. Azuelos, K. Benslama, D. Costanzo, G. Couture, J. Garcia, et al., Eur.Phys.J. **C39S2**, 13 (2005), hep-ph/0402037.
[61] A. Djouadi and G. Moreau, Phys.Lett. **B660**, 67 (2008), 0707.3800.
[62] A. Djouadi, G. Moreau, F. Richard, and R. K. Singh, Phys.Rev. **D82**, 071702 (2010), 0906.0604.
[63] A. Djouadi, G. Moreau, and F. Richard, Phys.Lett. **B701**, 458 (2011), 1105.3158.
[64] A. Azatov, M. Toharia, and L. Zhu, Phys.Rev. **D82**, 056004 (2010), 1006.5939.
[65] A. Djouadi, Phys.Lett. **B435**, 101 (1998), hep-ph/9806315.
[66] CMS web page, `https://twiki.cern.ch/twiki/bin/view/CMSPublic/PhysicsResults` (2012).
[67] ATLAS web page, `https://twiki.cern.ch/twiki/bin/view/AtlasPublic` (2012).
[68] ATLAS Collaboration (2012), 1202.1408.
[69] S. Chatrchyan et al. (CMS Collaboration) (2012), 1202.1488.
[70] M. Aliev, H. Lacker, U. Langenfeld, S. Moch, P. Uwer, et al., Comput.Phys.Commun. **182**, 1034 (2011), 1007.1327.
[71] S. Dittmaier et al. (LHC Higgs Cross Section Working Group) (2011), 1101.0593.
[72] S. Chatrchyan et al. (CMS Collaboration) (2012), submitted to Physics Letters B, 1203.5410.
[73] S. Chatrchyan et al. (CMS Collaboration), Phys.Rev.Lett. **107**, 271802 (2011), 1109.4985.
[74] G. Aad et al. (ATLAS Collaboration) (2012), 1202.3076.
[75] CERN Council Presentation, December 2011: `http://indico.cern.ch/conferenceDisplay.py?confId=164890` (2011).
[76] ATLAS Collaboration (2012), ATLAS-CONF-2012-019.
[77] R. Barbieri, L. J. Hall, Y. Nomura, and V. S. Rychkov, Phys.Rev. **D75**, 035007 (2007), hep-ph/0607332.
[78] L. Lavoura and J. P. Silva, Phys.Rev. **D47**, 2046 (1993).
[79] K. Nakamura et al. (Particle Data Group), J.Phys. **G37**, 075021 (2010).
[80] N. D. Christensen and C. Duhr, Comput.Phys.Commun. **180**, 1614 (2009), 0806.4194.
[81] M. Herquet and F. Maltoni, Nucl.Phys.Proc.Suppl. **179-180**, 211 (2008).
[82] T. Sjostrand, S. Mrenna, and P. Z. Skands, JHEP **05**, 026 (2006), hep-ph/0603175.
[83] S. Ovyn, X. Rouby, and V. Lemaitre (2009), 0903.2225.
[84] M. L. Mangano, M. Moretti, F. Piccinini, R. Pittau, and A. D. Polosa, JHEP **07**, 001 (2003), hep-ph/0206293.
[85] S. Chatrchyan et al. (CMS Collaboration) (2012), arXiv:1202.1487 [hep-ex].
[86] S. Chatrchyan et al. (CMS Collaboration) (2012), arXiv:1202.1997 [hep-ex].
[87] S. Chatrchyan et al. (CMS Collaboration) (2011), CMS-PAS-BTV-11-002.
[88] S. Catani, L. Cieri, D. de Florian, G. Ferrera, and M. Grazzini, Phys. Rev. Lett. **108**, 072001 (2012), URL `http://link.aps.org/doi/10.1103/PhysRevLett.108.072001`.
[89] A. Falkowski, Phys.Rev. **D77**, 055018 (2008), 0711.0828.
[90] J. Espinosa, C. Grojean, and M. Muhlleitner, JHEP **1005**, 065 (2010), 1003.3251.
[91] F. Ledroit, G. Moreau, and J. Morel, JHEP **0709**, 071 (2007), hep-ph/0703262.
[92] S. Casagrande, F. Goertz, U. Haisch, M. Neubert, and T. Pfoh, JHEP **1009**, 014 (2010), 1005.4315.
[93] The single production becomes dominant typically around $m_{t'} \sim 700$ GeV as in the scenario with a singlet t' [41] or in little Higgs models [60].
[94] Note that adding the contribution of the t' single production would increase the Higgs production rate.
[95] t' representations (to which SM fields are promoted) with analog rate suppression effects can arise with the O(3) subgroup [20] implementable in the composite Higgs model [89, 90] and RS scenario [91, 92] which can reach strong suppressions, respectively of $\sigma_{gg\to h}/\sigma^{SM}_{gg\to h} \sim 35\%$ and $\sim 10\%$.
[96] Such a heavy Higgs would be neither SM-like, as disfavored by the EW precision tests, nor belonging to a supersymmetric extension, as forbidden by the Higgs sector structure. However, it could perfectly be e.g. in a RS scenario where its contributions to the oblique T parameter can be compensated by new KK-induced contributions.
[97] The top quark exchange in the loop is the dominant contribution in the SM.
[98] Similar results are expected in such a situation.
[99] Namely the last two lines and columns of this mass matrix.
[100] We have also checked that the Tevatron constraints are satisfied.
[101] We thank Claude Duhr and Benjamin Fuks for their precious help in this implementation.